LoI May 2015

Compton Edge probing basic physics at JLab: light speed isotropy and Lorentz invariance

V.Gurzadyan[1,2], D.Gaskell[3], C. Keppel[3], A.Margaryan[1], D. Dutta[4], B. Vlahovic[2], S.Wood[3]

1. Alikhanian National Laboratory, Yerevan, 0036, Armenia
2. NASA University Research Center for Aerospace Device, NCCU, Durham, NC, 27707, US
3. Thomas Jefferson National Accelerator Facility, Newport News, VA, 23606, US
4. Mississippi State University, P.O. Drawer 5167, MS, 39762, US

Contacts: V. Gurzadyan, gurzadyan@yerphi.am, D. Gaskell, gaskelld@jlab.org

Abstract

High precision testing of basic physical principles, among those the light speed isotropy and the Lorentz invariance were always been major goals of experimental projects, both of dedicated ones and performed within other specialized studies. The reason is natural, i.e. consequences of detections of possible violations or deviations from those principles will have direct impact on the micro and macro physics, including cosmology. It is particularly remarkable that, the development of Lorentz invariance violating models has become a well established and active area of research, with periodical conferences and numerous publications, including proceedings volumes and monographs. The recent profound observations in cosmology, i.e. on the accelerated expansion of the Universe and the dark energy, dark matter and the cosmic microwave background tiny features, have made even more important the high accuracy testing of Lorentz invariance violating models.

We propose the study of the light speed isotropy and Lorentz invariance at Jefferson National Laboratory by means of the measurements of the Compton Edge (CE). This method, i.e. the studies of the daily variations of CE at the Compton scattering of high energy electrons with monochromatic laser photons for this purpose originally suggested in 1996 by Gurzadyan and Margaryan, later has been elaborated at GRAAL experiment at European Synchrotron Radiation

Facility (ESRF) in Grenoble. The obtained results for one-way speed of light isotropy and Lorentz invariance violation coefficients, became a reference number for various extensions of Special Relativity and related space-time fundamental issues.

The performing of the CE studies using 12GeV beam in JLab will enable the increase up to an order of magnitude of the currently available values for the mentioned limits, with direct impact on theoretical models in fundamental physics and cosmology.

1. Introduction

The importance of probing of the accuracy of basic physical principles, the Lorentz invariance and the light speed isotropy, was stated by Einstein in 1927 [1], i.e. far after the classical Michelson-Morley experiment and the formulation of the Special Relativity. Since then, such studies were continuously in the agenda of various experiments, e.g. [2-7], parallel to the active theoretical studies of corresponding models i.e. extensions of the standard model [8-10]; for extensive references both on the experiment and theory see http://en.wikipedia.org/wiki/Modern_searches_for_Lorentz_violation.

The recent indications of the dark energy in the Universe and the active search of the B-mode polarization of cosmic microwave background (CMB) have increased the interest to models with varying physical constants, including the speed of light, violation of the Lorentz, CPT invariance, e.g. [11,12].

The Compton Edge method first suggested in [13] includes the high precision daily measurements at the scattering of monochromatic accelerated electrons and laser photons, and which is crucial thus is tracing the one-way light speed. For comparison, majority of performed measurements of the light speed isotropy including the Michelson-Morley one, were dealing with a closed path propagation of light (see [2-7] and references therein). Such round-trip propagation are insensitive to the first order but are sensitive only to the second order of the velocity of the reference frame of the device with respect to a hypothetical universal rest frame. Mossbauer-rotor experiments yield a one-way limit $\Delta c/c < 2\ 10^{-8}$ [3], using fast beam laser spectroscopy. The latter using the light emitted by the atomic beam yield a limit $\Delta c/c < 3\ 10^{-9}$ for the anisotropy of the one-way velocity of the light. Similar limit was obtained for the difference in speeds of the uplink and the downlink signals used in the NASA GP-A rocket experiment to test the gravitational redshift effect [2]. One-way measurement of the speed of light has been performed using also NASA's Deep Space Network [8]: the obtained limits yielded $\Delta c/c < 3.5\ 10^{-7}$ and $\Delta c/c < 2\ 10^{-8}$ for linear and quadratic dependencies, respectively. Another class of experiments dealt not with angular but frequency dependence of the speed of light, as well the light speed dependence on the energy, using particularly the emission detected from the distant gamma sources, see the quoted Wikipedia article for extensive and recent references.

The Compton Edge (CE) method for this aim was first elaborated at the GRAAL facility in European Synchrotron Radiation Facility (ESRF) in Grenoble [14-17] using theelectron beam of 6 GeV. The final limit obtained there based on the dedicated measurements of 2008 yields $\Delta c/c=10^{-14}$. This result is currently used as a reference number to constrain various classes of theoretical models, thus proving both the experimental feasibility and theoretical importance of the task.

Further lowering of that limit at the measurements at Jefferson National Laboratory will enable to exclude certain models and pose constraints on the parameters of the others, with direct impact both on the models of dark energy, early evolution of the Universe and the interpretation of the observational/cosmological data regarding the fundamental physical principles.

We propose to perform measurements to probe the Lorentz invariance violation using the measurements of the Compton Edge at JLab, to obtain a lower limit than the currently available one, in view of the forthcoming 12 GeV electron beam energy.

The study of the light speed anisotropy using the Compton Edge method with respect to the dipole of the cosmic microwave background radiation, as the modern analog of the Michelson-Morley experiment, is also linked with the determination of the hierarchy of inertial frames and their relative motions, and is defining an "absolute" inertial frame of rest, i.e. the one where the dipole and quadrupole anisotropies vanish.

Namely, the dipole anisotropy of the temperature T of CMB is of Doppler nature [18],

$$\frac{\delta T(\theta)}{T} = (v/c)\cos\theta + (v^2/2c^2)\ \cos 2\theta + O(v^3/c^3) \qquad (1)$$

(the first term in the right hand side is the dipole term) and is indicating the Earth's motion with velocity

$$v/c = 0.000122\ \pm 0.00006;\ \ v = 365 \pm 18\, km/s, \qquad (2)$$

with respect to the above mentioned CMB frame. WMAP satellite [18] defines the amplitude of the dipole 3.346±0.017 mK and the coordinate of the apex of the motion (in galactic coordinates)

$$l = 263.85\ \pm 0.1;\ \ b = 48.25 \pm 0.04. \qquad (3)$$

This coordinate is in agreement with estimations based on the hierarchy of motions involving the Galaxy, the Local group and the Virgo super cluster [19].

The probing of the anisotropy of the speed of light with respect to the direction of CMB dipole, therefore, is a profound aim.

The organization of this document is as follows. First we review some of the classes of the Lorentz invariance violating models which have been directly affected by the GRAAL results. Then we outline the Compton Edge method, and the spectrometer. The GRAAL measurements are reviewed thereafter. The expected results and their discussion conclude the document.

2. Impact on fundamental theory and cosmology

Theoretical studies, including string theory and extensions of Special and General Relativities, predict violation of Lorentz invariance (see e.g. [8-10] and references therein). Various experimental studies, including using astronomical sources, have been conducted to probe the limits of those basic principles, since the increase in the accuracy of the available experimental limits will have direct impact for excluding of particular theoretical models or constraining the parameters of the others.

Here, for illustration, we mention several theoretical studies which are crucially based on the GRAAL experimental results; far more references can be found in the quoted articles.

2.1 Robertson-Mansouri-Sexl model.

One of often discussed extensions Special Relativity is the model suggested by Robertson and Mansouri and Sexl (RMS), dealing with the generalization of the transformation from one inertial frame to another including the spatial anisotropy and angular dependence of the speed of light. In that model the one-way velocity of light as measured in the inertial frame in which the laboratory is at rest can be written as (see [20])

$$c(v,\theta) = c[1-(1+2\alpha)(v/c)\cos\theta + O(v^3/c^3)], \tag{4}$$

where α=1/2 for the Special Relativity.

Below is a Figure from the review [20] on RMS light speed isotropy and Lorentz violating model vs the increase of the accuracy of the experiments. The one-way experiments of the GRAAL type are particularly important for testing of this popular extension of the Special relativity models and estimating the so-called Robertson-Mansouri-Sexl coefficients.

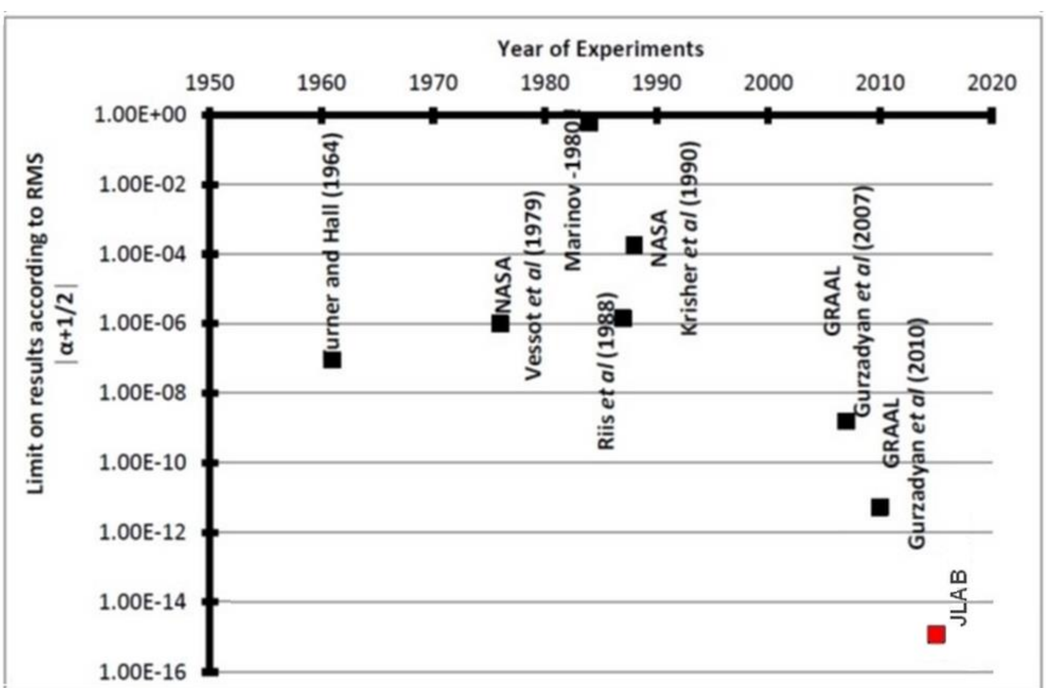

Fig. 1.This Figure reproduced from [20] exhibits the accuracy of the Robertson-Mansouri-Sexl coefficients obtained at various experiments. Einstein's Special theory of relativity corresponds to $|\alpha+1/2|= 0$. The red square is added here to denote the position of the expected result of JLab measurements as described in the current proposal.

2.2 GRAAL results vs Standard Model Extensions (SME)

In [21] the azimuthal dependence of the GRAAL data has been used for the diagnosis of a Standard Model Extension **(**SME) with space-time anisotropy, see the Fig. 2 below.

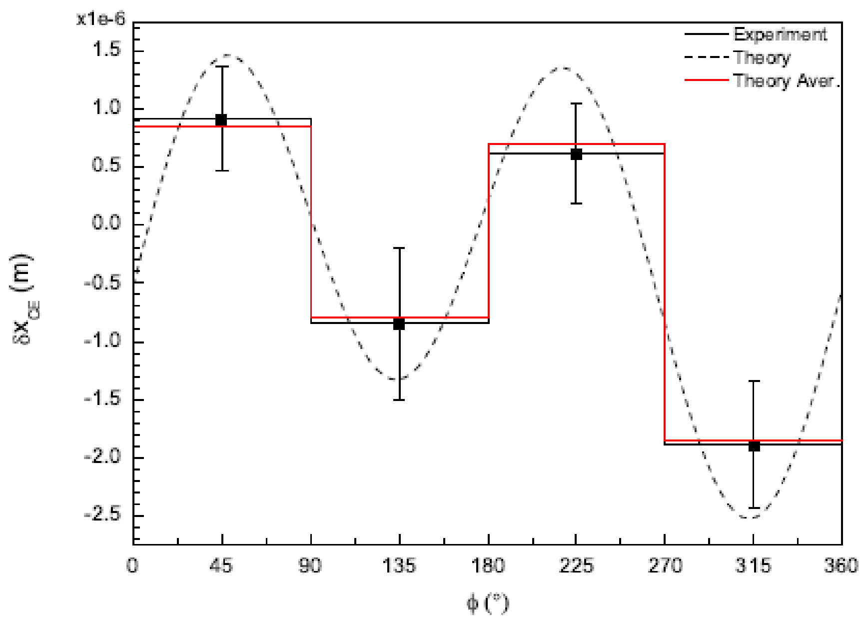

Fig. 2.δx_{CE} azimuthal distribution vs angles of the GRAAL data of the year 2008 on a plane (*x*-*y* plane or $\theta=\pi/2$),$\xi = 3.64 \times 10^{-13}$, $\lambda = 8.24 \times 10^{-14}$; this Figure is from [21].

On the one hand, the fit In the Figure 2 of the model with GRAAL data does not indicate much since the apparent variations in data are not statistically significant.

On the other hand, the unknown systematics in GRAAL experiments not allowing the further study of those apparent variations in the CE data can be overcome only at further increase of the accuracy of the measurements.

The principal conclusion is that, as one can see from Fig. 2, 4-fold increase in the accuracy, especially, by another facility, JLab, thus removing the instrumental systematics and will already be decisive for this model, either confirming the theoretically predicted variations or revealing their nature as of instrumental or other systematics.

2.3. Minimal standard model extension: Finslerian photon sector

The GRAAL results have been used also for obtaining of the constraints on the parameters of minimal standard model extension. Namely, in the minimal standard model extension (SME) the Lorentz-breaking Lagrangian of the pure photon sector is given by [22]

$$\mathcal{L}_{\text{photon}} = -\frac{1}{4}\eta^{\mu\rho}\eta^{\nu\sigma}F_{\mu\nu}F_{\rho\sigma} + \mathcal{L}_{\text{photon}}^{\text{CPT-even}} + \mathcal{L}_{\text{photon}}^{\text{CPT-odd}}, \tag{5}$$

where

$$\mathcal{L}_{\text{photon}}^{\text{CPT-even}} = -\frac{1}{4}(k_F)^{\mu\nu\rho\sigma}F_{\mu\nu}F_{\rho\sigma}, \tag{6}$$
$$\mathcal{L}_{\text{photon}}^{\text{CPT-odd}} = \frac{1}{2}(k_{AF})_{\alpha}\epsilon^{\alpha\beta\mu\nu}A_{\beta}A_{\mu\nu}. \tag{7}$$

The Lorentz invariance breaking parameter acquires an upper limit based on the GRAAL result

$$\sqrt{((\tilde{\kappa}_{o+})^{23})^2 + ((\tilde{\kappa}_{o+})^{31})^2} < 1.6 \times 10^{-14} \quad (95\% \text{ C.L.}) \tag{8}$$

2.4 Lorentz invariance violation with massive vector particles.

Among the growing activity on Lorentz invariance violating models, which will be directly influenced by the proposed measurements, we mention the class of Standard-Model Extensions (SME) with massive vector particles violating Lorentz and CPT invariance, given by the Lagrangian [23]

$$\mathcal{L}_{\gamma} = -\frac{1}{4}F^2 - A\cdot j - \frac{1}{4}F_{\kappa\lambda}\left(\hat{k}_F\right)^{\kappa\lambda\mu\nu}F_{\mu\nu} + \frac{1}{2}\epsilon^{\kappa\lambda\mu\nu}A_{\lambda}\left(\hat{k}_{AF}\right)_{\kappa}F_{\mu\nu}. \tag{9}$$

This extension is not only of interest for phenomenology of gauge bosons but also for Chern-Simons gravity emerging from string theory. The Chern-Simons gravity is among the models involved to explain the dark energy observational data.

2.5 B-mode cosmology and the break of Lorentz invariance

The detection of B-mode polarization will have major consequences not only for the studies of the early Universe but for the fundamental physical principles up to trans-Planck energies (cf. [11]). Among the theoretical models dealing with the scalar, tensor primordial fluctuations and the power spectrum of the temperature of the cosmic microwave background is the possible anti-correlation scalar and tensor modes via the Lorentz invariance violation [12]. The latter can be linked to large scale anomalies known in the temperature anisotropy defined by the two-point correlation function (for details and notations see [12])

$$C_{\mathrm{l}}^{\mathrm{corr}} = -\frac{\pi}{5}\frac{v^2}{\tau_0^2}\int \frac{dq}{k'^3} n^i n^j \prod_{ij}^{33}(k') = -\frac{\pi v^2}{75\,\mathrm{l}^4}\left(-l_x^2 + 5l_y^2 + 2\left(3l_x^2 + l_y^2\right)\cos 2\theta\right). \quad (10)$$

The Lorentz invariance here is reduced to the invariance of this correlator with respect to rotations, i.e. which in principle can be tested at cosmic microwave background temperature measurements. Any constraint on the Lorentz invariance violation from the CE measurements can be confronted with these data and the interpretations both in the cosmological evolution context and basic physical principles up to Planckian energies and even higher.

The mentioned examples do indicate that, the increase of accuracy of measurements performed in JLab, in certain cases already 4-fold, can be crucial either to rule out certain theoretical models or to reveal the nature of the angular-dependent variations in the GRAAL data, with direct consequences for quantum field theories and cosmology.

2.5 Lorentz violating dark matter and dark energy

Dark energy and dark matter inducing Lorentz invariance violation models have also been investigated, see e.g. [24-25] and references therein. In the model considered in [24] the low energy action for the scalar field has the form

$$S_{[\Theta]} = \int d^4 x\sqrt{-g}\left(-\frac{g^{\mu\nu}\partial_\mu\Theta\partial_\nu\Theta}{2} + \kappa\frac{\left(u^\mu\partial_\mu\Theta\right)^2}{2} - \mu^2 u^\mu\partial_\mu\Theta\right) \tag{11}$$

with the cosmological constant setting zero, and with the coupled field and the gravity of Einstein-Hilbert Lagrangian. Then the Friedmann equation has the form

$$H^2 = \frac{8\pi G_{cos}}{3}\left(\rho_\mu + \rho_s + \rho_d + \sum\nolimits_{\text{other}}\rho_n\right), \tag{12}$$

where

$$\rho_\mu \equiv \frac{\mu^4}{2(1+\kappa)}, \quad \rho_s \equiv \frac{C^2(1+\kappa)}{2a^6}, \quad \rho_d = -\frac{\mu^2 C}{a^3}, \tag{13}$$

and the density components under the sign of the sum denote the standard matter components (cold dark matter, photons, neutrinos). The rest refer to those of the scalar field described by the dynamical equation

$$\dot{\Theta} = -\frac{\mu^2 a}{1+\kappa} + \frac{C}{a^2}, \tag{14}$$

where C is the integration constant (for details see [24]). It is shown that the Lorentz violation, triggering a preferred direction in space-time, i.e. generating anisotropic stress, can be pronounced also in the evolution of cosmological perturbations, i.e. in the large scale effects.

In the case of dark matter the coupling part of the action has the form [25]

$$S_{[\text{DMu}]} = -m\int d^4x\sqrt{-g}\, n\, F\left(u_\mu v^\mu\right), \tag{15}$$

where *m* is the mass of the dark matter particles, *n* is the their number density and *v* is their 4-velocity, and the function *F* is entering the dynamical equations.. The extension of the special relativistic relation then reads

$$E^2 = m^2c^4 + (1+\xi)\mathrm{p}^2 \,, \tag{16}$$

where ξ=0 corresponds to the Lorentz invariance.

The common in these models is the spatial anisotropy due to the Lorentz invariance violation determined by the scalar field which can reveal itself in cosmological scale as either dark energy or dark matter, or other observable effects such as the cosmic microwave background, the large scale matter distribution features, see also [26, 27]. It is noted that the latter are solely due to the scalar perturbations while the vector ones can lead to B-mode effects.

These are examples of models of link of the Lorentz invariance violation and the dark sector – dark energy and dark matter – properties in the cosmological scales. These models do involve options in the Lorentz violation schemes each depending on defined parameters which themselves in each case at further specification can be constraint by the observational data on the cosmic background radiation, and the GRAAL type data or of future JLAB ones.   No doubt, other specific models based on Lorentz invariance violation will be developed in future as well, and therefore its experimental limits will in either case affect the understanding of the dark sector.

3 The Compton Edge method and its elaboration

The energy of the scattered photon ω_{21} is related to the energy of the primery laser photon ω_{01} by the equation

$$\omega_{21} = \frac{(1-\beta\cos\theta)\omega_{01}}{1-\beta\cos\theta_\gamma+(1-\cos\theta_0)(\omega_{01}/\mathrm{E}_1)} \,, \tag{17}$$

where E_1 and E_2 are the energies of the incident and scattered electron, $\beta = v/c$, v is the velocity of the incident electron, θ_0 is the angle between the momentum of incident and scattered photon, θ and θ_γ are angles between the momentum of the electron and incident and scattered photons, respectively, θ_e is the angle between the momentum of incident and scattered electron (see Fig. 3). Rewrite this expression in the following form

$$\omega_{21} = \omega_{01} A \gamma^2, \tag{18}$$

$$\gamma^2 = (1 - \beta^2)^{-1} \tag{19}$$

$$A = \frac{(1-\beta\cos\theta)(1+\beta\cos\theta_\gamma)}{1+\beta^2\gamma^2\sin^2(\theta_\gamma)+\gamma^2(1-\cos\theta_0)(1+\beta\cos\theta_\gamma)(\omega_{01}/E_1)}. \tag{20}$$

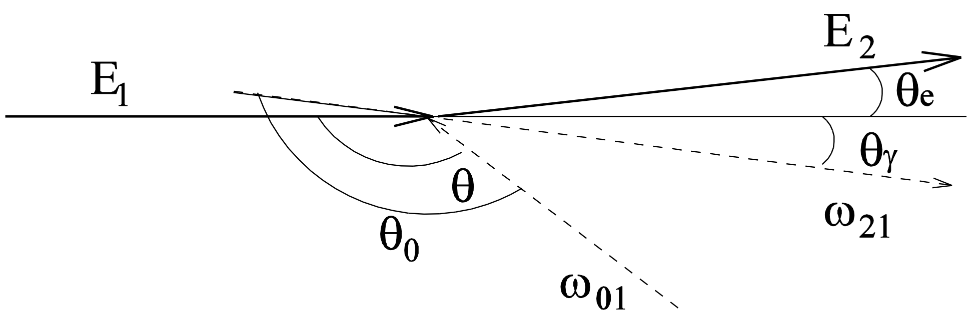

Fig. 3. The kinematics of Compton scattering.

The energy of the scattered photon at small angles $(\gamma\theta_\gamma) < 1$ up to $\gamma \sim 10^5$ is proportional to the square of the electron energy since the factor A depends on $\gamma \leq 10^5$ weakly.

Rewrite equation (18) in the following form [28]

$$\omega_{21} = \frac{\omega_{01}}{1+(\theta_\gamma/\vartheta_0)^2}, \tag{21}$$

$$\vartheta_0 = \frac{m_e c^2}{E_1}\sqrt{x+1}, \tag{22}$$

$$x = \frac{4E_1\omega_{01}\cos^2(\alpha/2)}{m_e^2 c^4}, \tag{23}$$

where $\alpha = \pi - \theta$.

The maximum energy of the scattered photon or the Compton Edge is given by

$$\omega_{21}^{max} = \frac{x}{x+1} E_1 \tag{24}$$

or

$$\omega_{21}^{\max} = \frac{4\gamma^2\omega_{01}}{x+1} \tag{25}$$

and

$$x = \frac{4E_1\omega_{01}}{m_e^2c^4} \tag{26}$$

which is obained for 180° scattering in head-on collision

$\theta = \theta_0 = \pi$ and $\theta_\gamma = 0$.

For example: E_1= 6.0 GeV, $\omega_{01} = 3.54$ eV (Argon ion laser) $x = 0.325$ and $\omega_{21}^{max} = 0.254E1$.

The photon and electron scattering angles are functions of the photon energy

$$\theta_\gamma(y_\gamma) = \vartheta_0\sqrt{\frac{y_\gamma^{\max}}{y_\gamma} - 1}, \tag{27}$$

$$\theta_e(y_\gamma) = \theta_\gamma \frac{y_\gamma}{1-y_\gamma}, \tag{28}$$

where $y_\gamma = \omega_{21}/E_1$. These functions for $x = 0.325$ are displayed in Fig. 4.

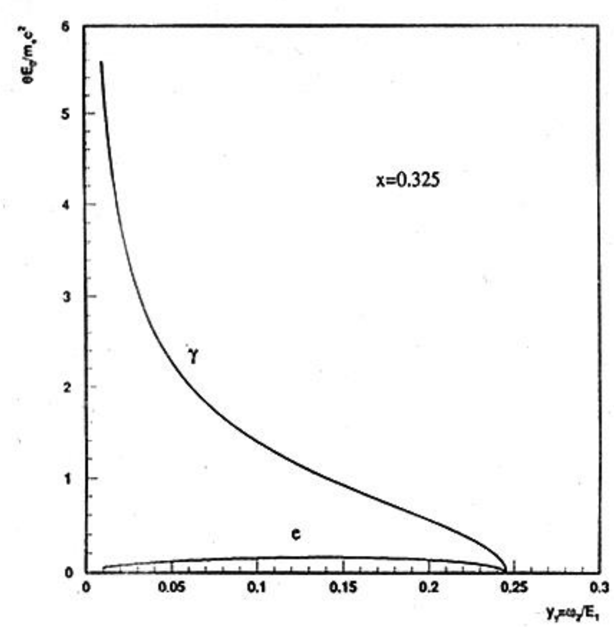

Fig. 4. Electron and photon scattering angles vs photon energy for $x = 0.325$; Figures 4 -10 are from [29].

The energy spectrum of the scattered photons is defined by the cross section

$$\frac{1}{\sigma_c}\frac{d\sigma_c}{dy_\gamma} \equiv f(x, y_\gamma) = \frac{2\sigma_0}{x\sigma_c}\left(\frac{1}{1-y_\gamma} + 1 - y_\gamma - 4r(1-r)\right), \quad (29)$$

where

$$y_\gamma \le y_\gamma^{max} = \frac{x}{x+1}; \quad (30)$$

$$r = \frac{y_\gamma}{x(1-y_\gamma)} \le 1; \quad (31)$$

$$\sigma_0 = \pi\left(\frac{e^2}{m_e c^2}\right)^2 = 2.5 \times 10^{-25} cm^2. \quad (32)$$

The total Compton cross section for the nonpolarized case is

$$\sigma_c = \frac{2\sigma_0}{x}\left(\left(1 - \frac{4}{x} - \frac{8}{x^2}\right)\ln(x+1) + \frac{1}{2} + \frac{8}{x} - \frac{1}{2(x+1)^2}\right). \quad (33)$$

The absolute value of the energy of incident electrons can be determined by the measurement of the absolute value of the Compton edges of scattered electrons or photons as well as by means of the determination of the rations: 1. $y_e^{min} = E_{21}^{min}/E_1$; 2. $y_\gamma^{max} = \omega_{21}^{max}/E_1$; 3. $a_e = E_{21}^{min}/E_{22}^{min}$; 4. $a_\gamma = \omega_{22}^{max}/\omega_{21}^{max}$, where E_{21}^{min}, E_{22}^{min}, $(\omega_{21}^{max}, \omega_{22}^{max})$ are the values of Compton Edges of scattered electrons (photons) from two different laser lines $(\omega_{01}, \omega_{02})$ and $y_e = 1 - y_\gamma$; $y_e^{min} = 1 - y_\gamma^{max} = 1/(1+x)$ [29].

For example in the case of 2 and 3 we have

$$x = \frac{y_\gamma^{max}}{1-y_\gamma^{max}} \quad (34)$$

and

$$x = \frac{1-a_e}{a_e(1-\omega_{02}/\omega_{01})}. \quad (35)$$

The energy spectra of the scattered photons and electrons for $x = 0.325$ are displayed in Fig. 5 and Fig. 6, respectively.

However the test of the one-way light speed isotropy can be cheked only by precise measurement of the relative changes of Compton Edge as was done at GRAAL.

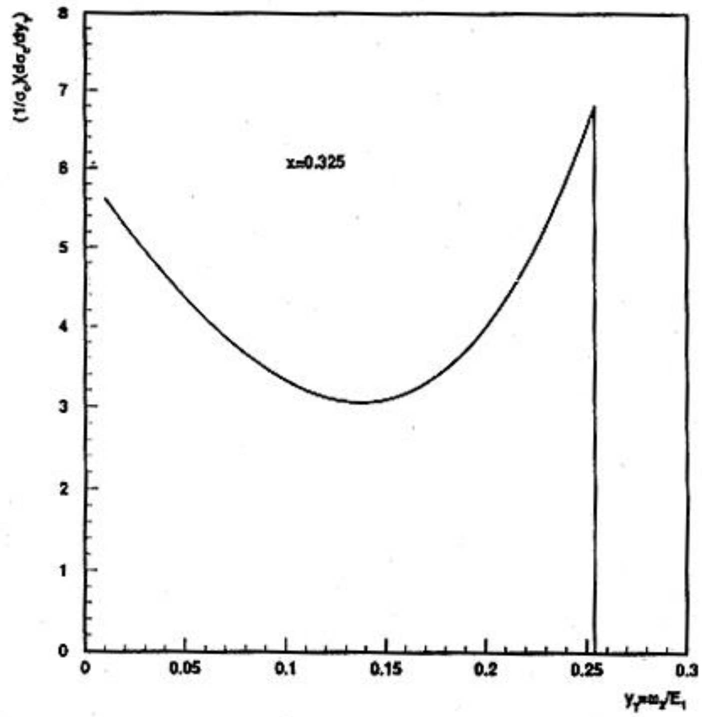

Fig. 5. Energy spectra of scattered photons for $x = 0.325$. The energy is in units of ω_{21}/E_1.

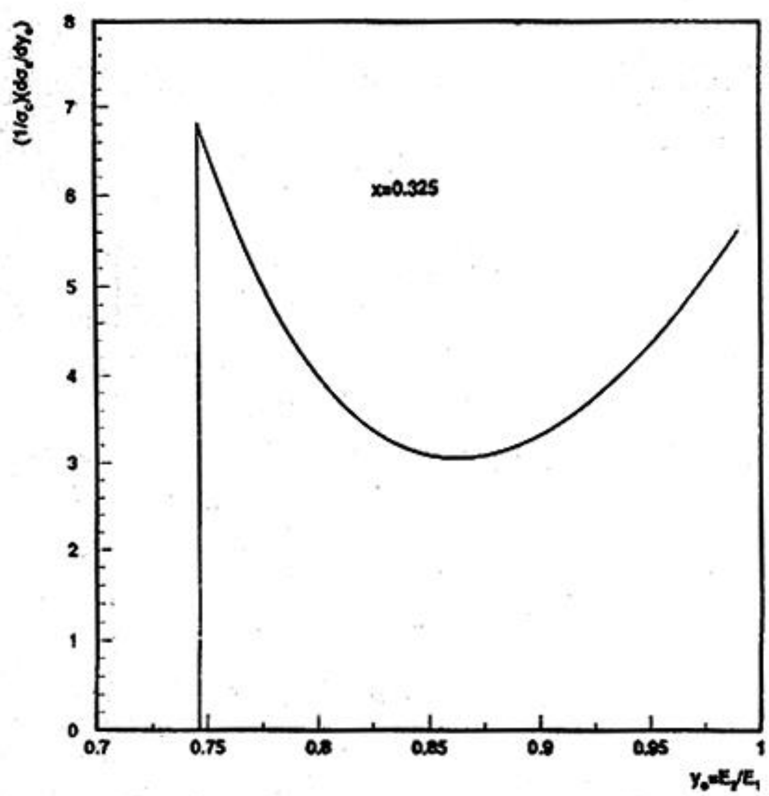

Fig. 6. Energy spectra of scattered electrons for $x = 0.325$. The energy is in units of $E_{21/}E_1$.

4 The test of the one-way light speed isotropy

If the energy of the ultra-relativistic electron beam is kept stable with given accuracy, namely the beam energy is stable over a long time and not at an instantaneous measurement, the Compton Edge variation will result in the estimation of forward scattered light speed variation

$$\beta\, d\beta = \left(\frac{1}{\gamma^2}\right)\frac{d\gamma}{\gamma}\ . \tag{33}$$

The error in β is reduced by a factor $(1/\gamma^2)$ with respect to the Compton Edge or beam energy error. For CEBAF ($E = 11$ GeV, $\delta E/E < 3{\times}10^{-5}$ [30]) one has $d\beta = 6{\times}10^{-14}$. The error of mean values of β measured by this way should be even on 1-2 orders of magnitude improved.

To chek the directional sensitivity of the Compton Edge rewrite formula (17):

$$\omega_{21} = \frac{(1-\beta_2\cos\theta)\omega_{01}}{1-\beta_1\cos\theta_\gamma+(1-\cos\theta_0)(\omega_{01}/E_1)}\quad . \tag{34}$$

Where $\beta_1 = v/c_1$, $\beta_2 = v/c_2$ and c_2, c_1 are speeds of the laser and scattered photons respectively. In the spacial relativity $c_1 = c_2 = c$ and $\beta_1 = \beta_2 = \beta = v/c$.

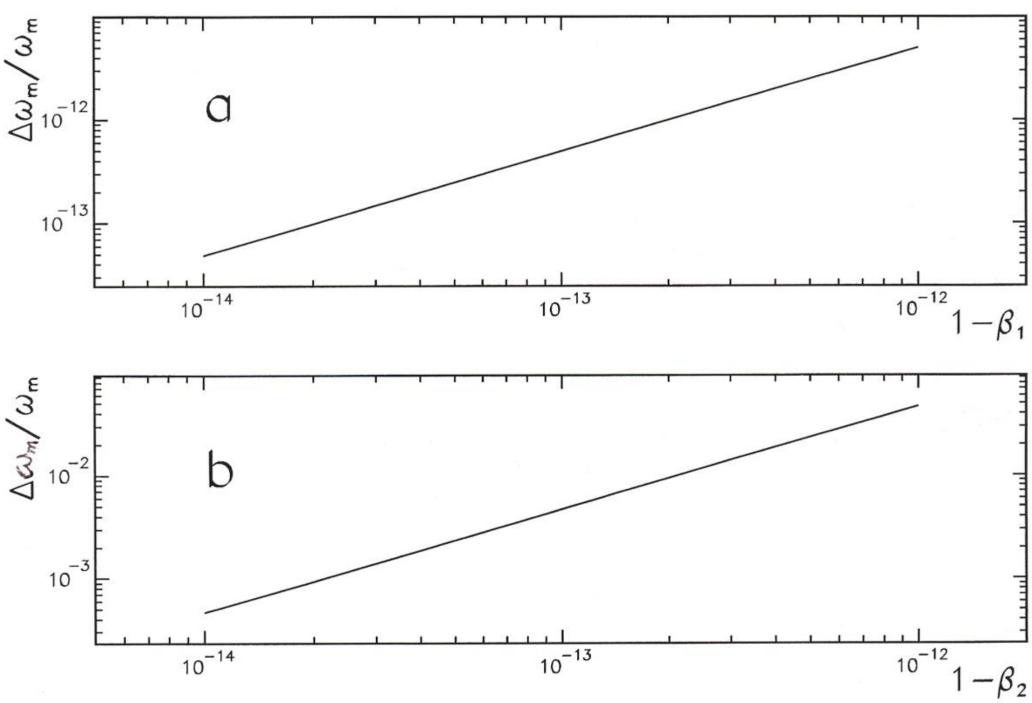

Fig. 7. The variation of the Compton Edge against β_1 (a) and β_2 (b).

In Fig. 7 the variations of the Compton Edge ω^{max} in head-on collisions against the β_1 and β_2 are presented. One can see that trhe ω^{max} practically is sensitive to the variation of the β_2. Therefore, the kinematics of the Compton scattering of high energy electrons, i.e. of high Lorentz factor, and laser photons can be used for tracing of the one way light speed isotropy limit [13]. The measurement with respect to the dipole of the cosmic microwave background radiation, as of a rest frame i.e. when the dipole anisotropy is vanishing, shows the analogy with the Michelson-Morley experiment; the motion with respect to CMB defines the hierarchy of motions that the Earth is participating in [19].

5 Results of Monte Carlo Simulations of the Compton Edge Spectrometer

The main idea of this method based on the inclusive energy spectrum measurement near the kinematical (Compton) edge of electrons scattered on the laser photons. In this paragraph we present the results of Monte Carlo simulations of such spectrometer. These calculations were carried in the framework of the two body kinematics, by using of the formula (29). We consider the absolute energy determination of the electron beams of GRAAL [32], CEBAF [33, 34], and SLC [35] electron accelerators.

The error (FWHM) of the Compton edge of the GRAAL and CEBAF facilities ($E_1 = 6000\,MeV$) are 15 MeV and 3 MeV, respectively. These values include all the effects due to the electron beam phase space and energy resolution of the recoil electron spectrometer (tagged system). For the error of the Compton edge of the SLC electron beam ($E_1 = 50000\,MeV$) we used the value of 150 MeV, which include only the effect of the energy dispersion of incident electron beam($FWHM/E_1 = 3 \times 10^{-3}$). The expected energy distribution of scattered electrons near Compton Edges, obtained by Monte Carlo simulations, for GRAAL, CEBAF and SLC are presented in Fig. 8, 9, 10. The corresponding laser frequencies for GRAAL, CEBAF and SLC are 3.54, 3.54 and 1.17 eV, respectively. The total number of events is 2×10^5.

Fitting the Monte Carlo spectrum presented in Fig. 8- Fig. 10 by the convolution of the resolution function with the theoretical cross section, using a fitting algorithm based on Gaussian statistics, 6000 ± 0.09 MeV, 6000 ± 0.06 MeV and 49999 ± 2.9 MeV with an effective χ^2 per degree of freedom of 0.90, 0.98 and 1.28 can be extracted respectively. The obtained results are presented in Table 1.

Table 1. The used parameters and extracted values of the GRAAL, CEBAF and SLC beam energies and the dispersions obtained with the help of Eq.7.

Device	E_1 MeV	FWHM MeV	ω_{01} eV	E_1^{fit} MeV	χ^2/NDF
CEBAF	6000	3.0	1.17	6000.0$\pm$0.025	1.04
	6000	3.0	3.54	6000.0$\pm$0.060	0.98
GRAAL	6000	15.0	1.17	6000.0$\pm$0.500	1.35
	6000	15.0	3.54	6000.0$\pm$0.090	0.90
SLC	50000	150.0	1.17	49999.0$\pm$2.9	1.28
	50000	150.0	2.34	49997.0$\pm$7.0	1.20

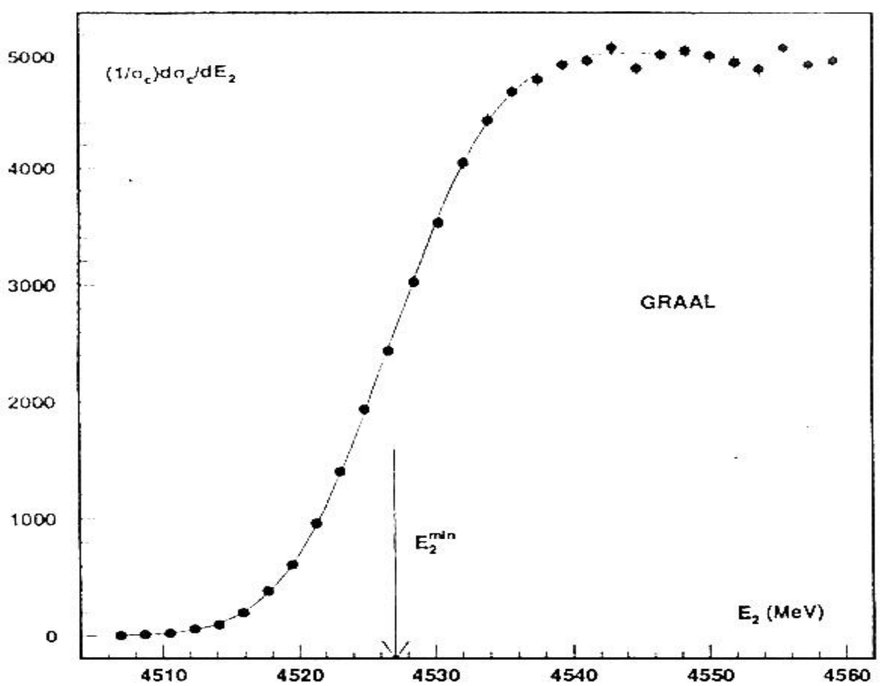

Fig. 8. Energy spectrum of scattered electrons near Compton edge. The data show the MC simulation result, the curve is a result of the fit. The extracted electron beam energy is 6000.0$\pm$ 0.090 with a true beam energy 6000 MeV and laser photon energy 3.54 eV.

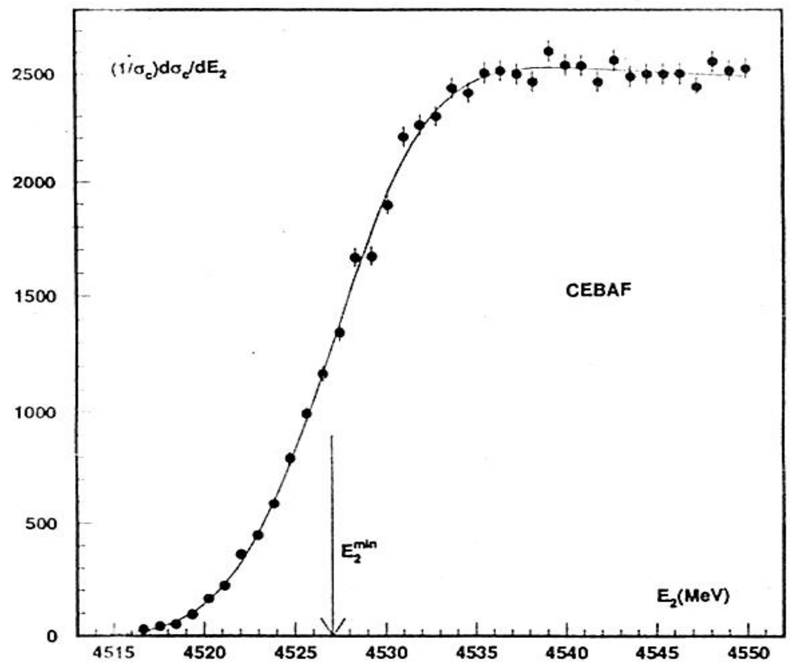

Fig. 9. The same as in Fig 5 but for CEBAF electron beam. The extracted electron beam energy is 6000.0 ± 0.060 MeV with a true beam energy 6000 MeV and laser photon energy 3.54 eV.

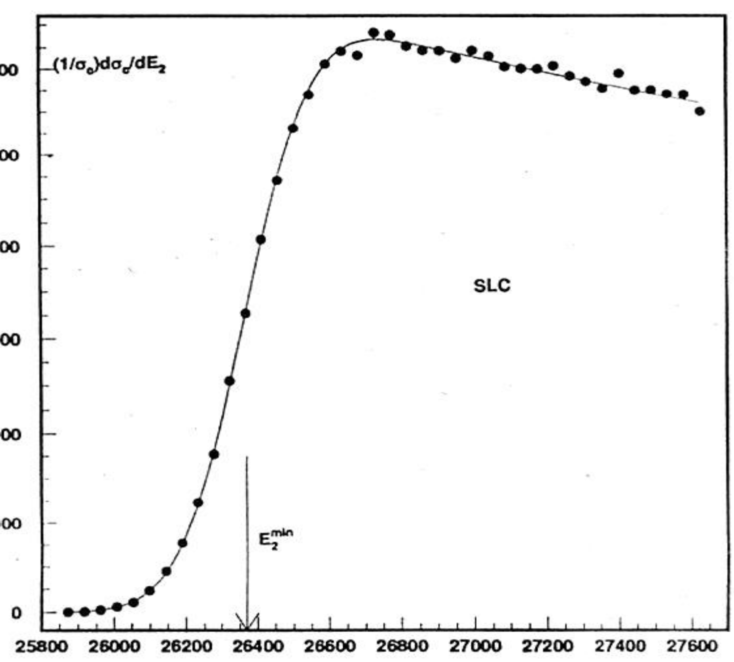

Fig. 10. The same as in Fig. 5 but for SLC electron beam. The extracted electron beam energy is 49999.0 ± 2.9 MeV with a true beam energy 50000 MeV and laser photon energy 1.17 eV.

6 GRAAL/ESRF: the Experimental Setup and measurements

The measurement of the Compton Edge of the scattered high energy electrons of synchrotrons on monochromatic laser beams, has been originally suggested in [13] as an efficient test for the one-way light speed isotropy and the Lorentz invariance in the reference frame of the cosmic microwave background radiation. This method has been successfully elaborated at GRAAL facility at European Synchrotron Radiation Facility. Initially, the analysis of the data of 1998-2002 (non-continuous) measurements enabled to obtain an upper limit for the anisotropy 10^{-12} [14]. Then, dedicated measurements, i.e. with a facility upgraded for that particular goal, have been performed in 2008, which enabled to lower further that limit, up to 10^{-14} [15, 16].

In the experiment carried out with the GRAAL facility, installed at the European Synchrotron Radiation Facility (ESRF), the γ-ray beam was produced by Compton scattering of laser photons off the 6.03 GeV electrons circulating in the storage ring. Incoming photons are generated by a high-power Ar laser located about 40 m from the intersection region. The laser beam enters the vacuum via an MgF window and is then reflected by an Al-coated Be mirror towards the electron beam. The laser and electron beams overlap over a 6.5 m long straight section. Photons are finally absorbed in a four-quadrant calorimeter, which allows the stabilization of the laser-beam center to 0.1 mm. This level of stability is necessary and corresponds to a major improvement of the updated set-up. Because of their energy loss, scattered electrons are extracted from the main beam in the magnetic dipole following the straight section. Their position can then be accurately measured in the tagging system (Fig. 11) located 50 cm after the exit of the dipole.

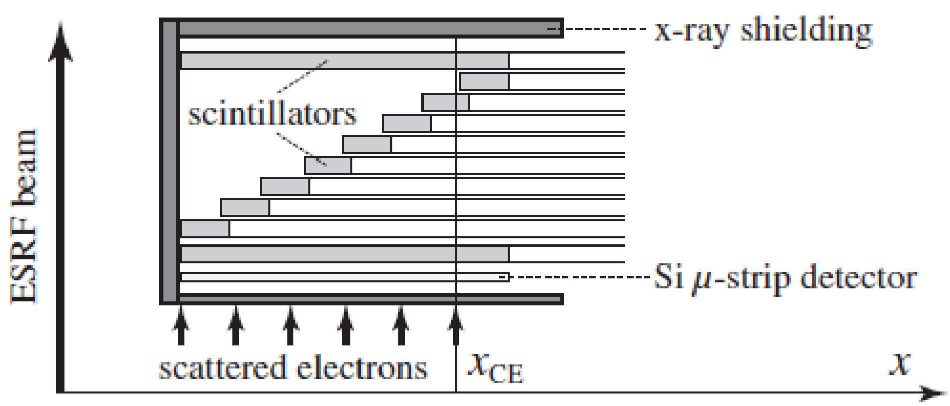

Fig. 11. The schematic of the GRAAL tagging system.

This system plays the role of a magnetic spectrometer from which we can infer the electron momentum. The tagging system is composed of a position-sensitive Si μ-strip detector (128 strips of 300 μm pitch, 500 μm thick) associated to a set of fast plastic scintillators for timing information and triggering of the data acquisition. These detectors are placed inside a movable box shielded against the huge x-ray background generated in the dipole. The x-ray induced heat load, which is the origin of sizable variations in the box temperature, correlated with the ESRF beam intensity. This produces a continuous drift of the detector due to the dilation of the box. A typical Si μ-strip count spectrum near the CE is shown in Fig. 12 for the green and multiline UV mode of the laser used in this measurement.

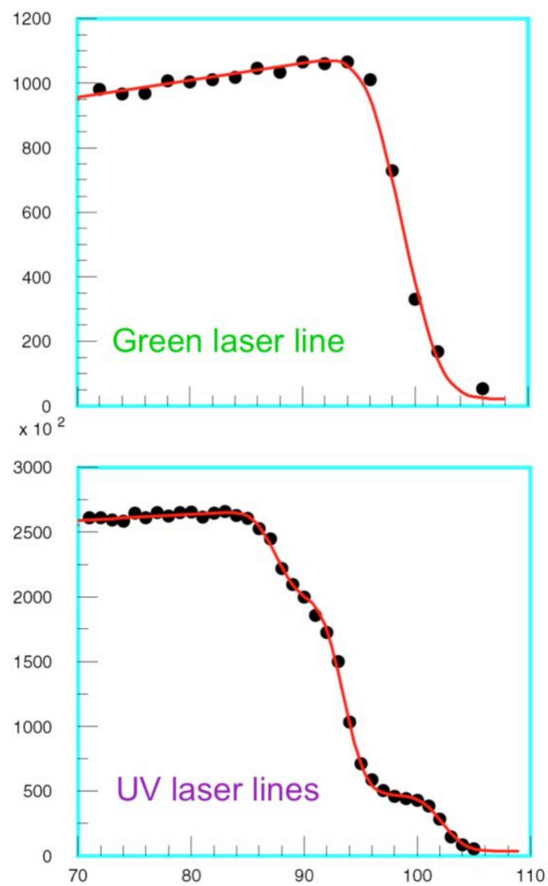

Fig. 12. The Compton Edge for the Green laser line (2.41 eV) and the lower one with three UV lines around 3.53 eV for the parameters of the GRAAL facility. The abscissa indicates the microstrip number.

The multiline UV mode (displayed separately in Fig. 13) corresponds to three groups of lines centered around 364, 351, and 333 nm, which are clearly resolved. The fitting function is also plotted in Fig. 13. The CE position, x_{CE}, is taken as the location of the central line. The steep slope of the CE permits an excellent measurement of x_{CE} with a resolution of ~3 μm for a statistics of about 10^6 counts.

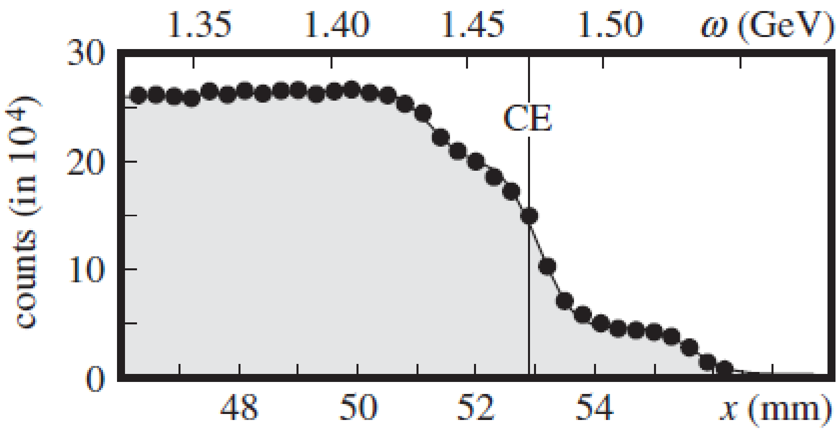

Fig. 13. Si μ-strip count spectrum near the CE and the fitting function vs position x and scattered photon energy ω.

During a week of data-taking in July 2008, a total of14 765 CE spectra have been recorded. A sample of the time series of the CE positions relative to the ESRF beam covering 24 h is displayed in Fig. 14. Fig. 14(c), along with the tagging-box temperature [Fig. 14(b)] and the ESRF beam intensity [Fig. 14(a)]. The sharp steps present in Fig. 14(a) correspond to the twice-a-day refills of the ESRF ring. The similarity of the temperature and CE spectra combined with their correlation with the ESRF beam intensity led to interpret the continuous and slow drift of the CE positions as a result of the tagging-box dilation. To remove this trivial time dependence, a special fitting procedure was developed. The corrected and final spectrum, obtained by subtraction of the fitted function from the raw data, is plotted in Fig. 14(d). A sample of such a spectrum is displayed separately in Fig. 15.

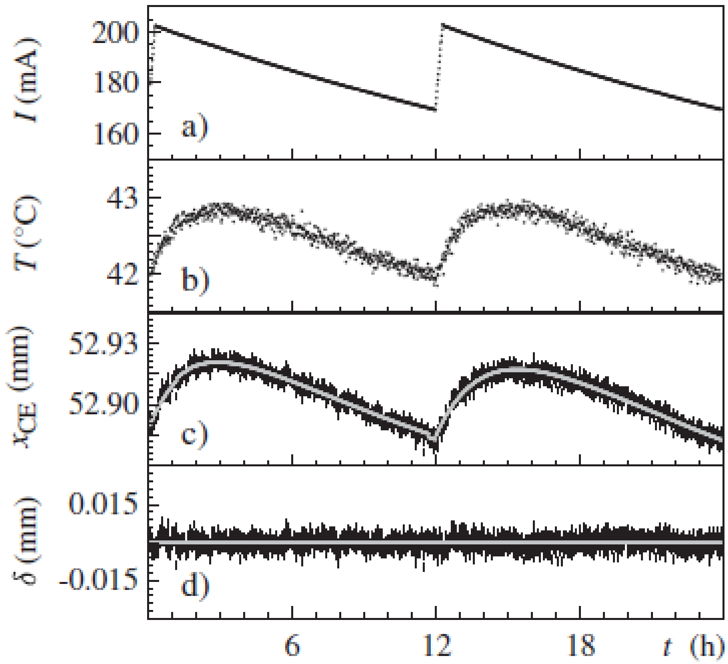

Fig. 14.Time evolution over a day of (a) ESRF beam intensity, (b) tagging-box temperature, (c) CE position and fitted curve, and (d) $\delta = x_{CE} - x_{fit}$. The error bars on position measurements are directly given by the CE fit.

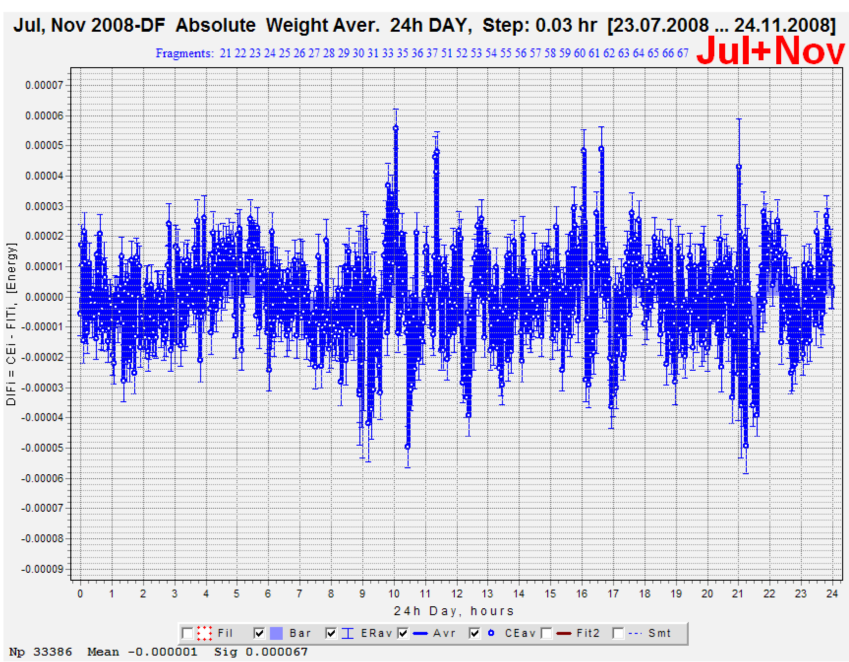

Fig. 15. The Compton Edge time variations obtained at GRAAL 2008 measurements.

The GRAAL collaboration presented an upper bound on a hypothetical sidereal oscillation of the CE energy to be less than 2.510^{-6} (95% C. L.) yielding the competitive limit on the one way light speed anisotropy to be less than 1.810^{-14} (95% C. L.).

We propose to carry out this experiment at JLAB by using 12 GeV electron beam and Hall A Compton polarimeter setup.We think that with a modified polarimeter, main ammount of data could be obtained working in parasitic mode, i.e. in this stage we are not requiring dedicated beam time. We expect to improve about order of magnitude the upper bound of the one way light speed anisotropy obtained at GRAAL. The parameters for the JLAB facility on the Compton electron detector are presented in Fig. 16 (D. Gaskell, 2014) [42].

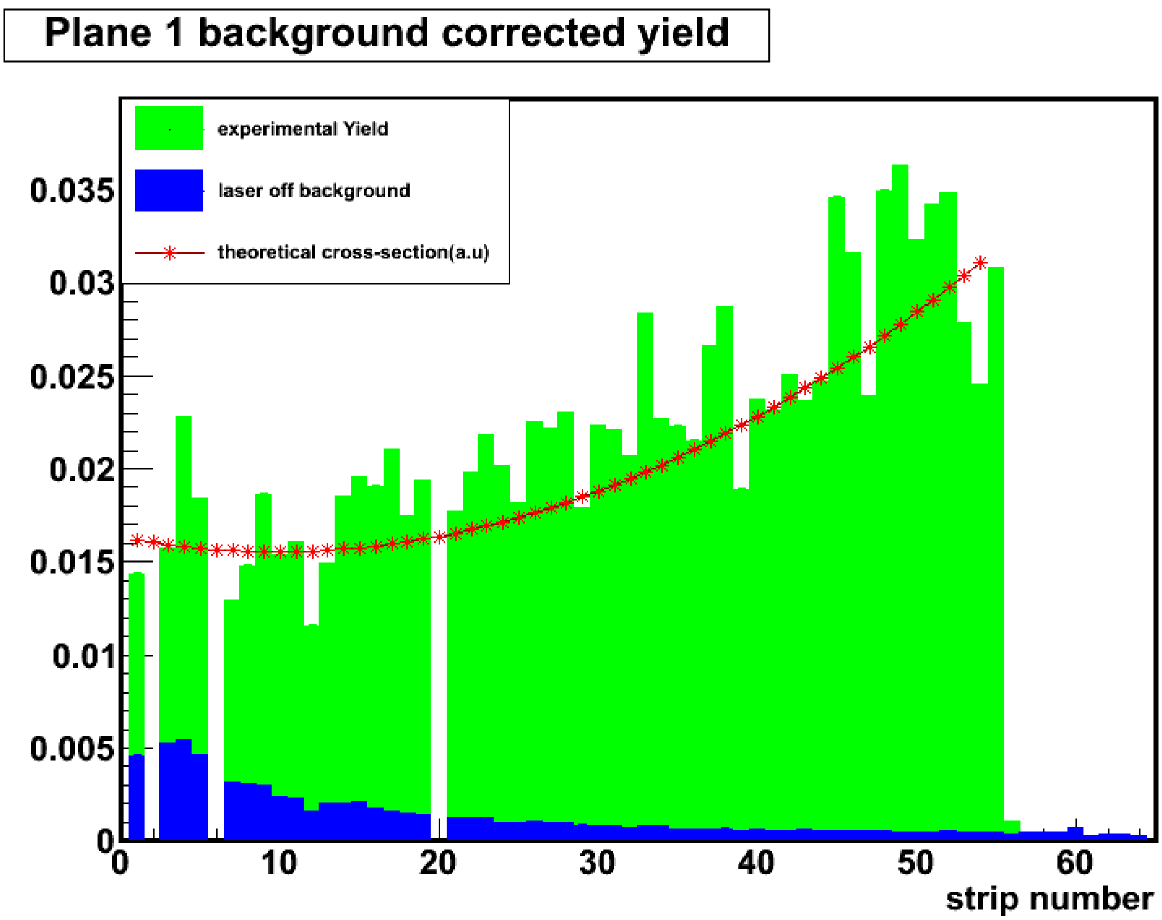

Fig. 16. Si strip count spectrum with theoretical cross section (a.u). Blue part is the laser of background. Strip number corresponds to scattered electron energy.

Conclusions

The main goals expected for this project can be summarized as follows:

1. Based on successfully performed GRAAL-ESRF measurements and the obtained results, the Compton Edge method has proved its efficiency for testing the fundamental physical principles, i.e. one-way light speed isotropy and the Lorentz invariance violation.
2. The Compton Edge studies on 12 GeV electron accelerator beam in Jefferson National Laboratory is feasible for the increase of the limits reached at GRAAL.
3. The expected results of higher accuracy of the Compton Edge **relative changes** will have direct impact on theoretical models of Lorentz invariance violation, will enable either to close certain models or obtain constraints on the parameters of the others. In outcome, the models will affect numerous fundamental physical problems including in cosmology and the evolution of the very early Universe.

The ongoing studies of the cosmic microwave background by ground based telescopes and Planck satellite and the forthcoming data for tracing up to the trans-Planckian scale of energies with the B-mode polarization, non-Gaussianities [11, 12, 36-39], dark energy redshift evolution (e.g. [40]), make more outlined this proposal besides the traditional interest for Lorentz invariance violating models.

To achieve the goal regarding the impact on fundamental physics this LoI is stating the need of: (a) electron and photon detectors ensuring the needed accuracy of the measurements, and (b) the beam time, both in view of the experience with GRAAL-ESRF, look feasible in JLab.

Then, two options are possible:

1. **use of the available detectors;**
2. **development of new detectors compatible with the precision polarization measurements required, which, certainly, will need some efforts.**

APENDIX

Practical Issues Concerning to Compton Edge Spectrometer

We consider the case of measuring of the energy distribution of recoil electrons near the Compton edge. Basically the method involves measuring the deflection of recoil electrons in a magnetic field. Therefore, this method requires measurement of the magnetic field integrals and the bending angles. In order to determine the beam momentum to 10^{-4}, both of these quantities must be determined at a level somewhat better than 10^{-4}. For SLC magnets, the attainable accuracy for the absolute value of the field integrals is of the order of 10^{-4} [31].

Since the Compton electron scattering angles are smaller ($\leq 10^{-5}$rad, see Fig. 4) than the angular divergence of the beam ($10^{-4} - 10^{-5}$), the scattered and unscattered electrons remain unsepareted until they pass through dipole magnets. Both beams are dispersed and recoil electrons detected (see Fig. 16).

To determine the bending angles of recoil electrons, position sensitive detector, e.g. silicon microstrip detector mounted on a precision optical table would be used. If center of the magnetic field is known and the distance between the center and magnetic field and monitors is c, the distance between the centroid of the forward scattered photons (and hence the centroid of the incident electron beam) and recoil electron is a, then the bend angle is $\vartheta = a/c$. Assuming the errors in these quantities are independent:

$$\frac{d\vartheta}{\vartheta} = \sqrt{\left(\frac{da}{s}\right)^2 + \left(\frac{dc}{c}\right)^2} \qquad (4.11)$$

Usually, c is of the orders of 10 m, a about 1 m, therefore to reach the precession better than 10^{-4} we will have $da = dc \leq 100\mu m$.

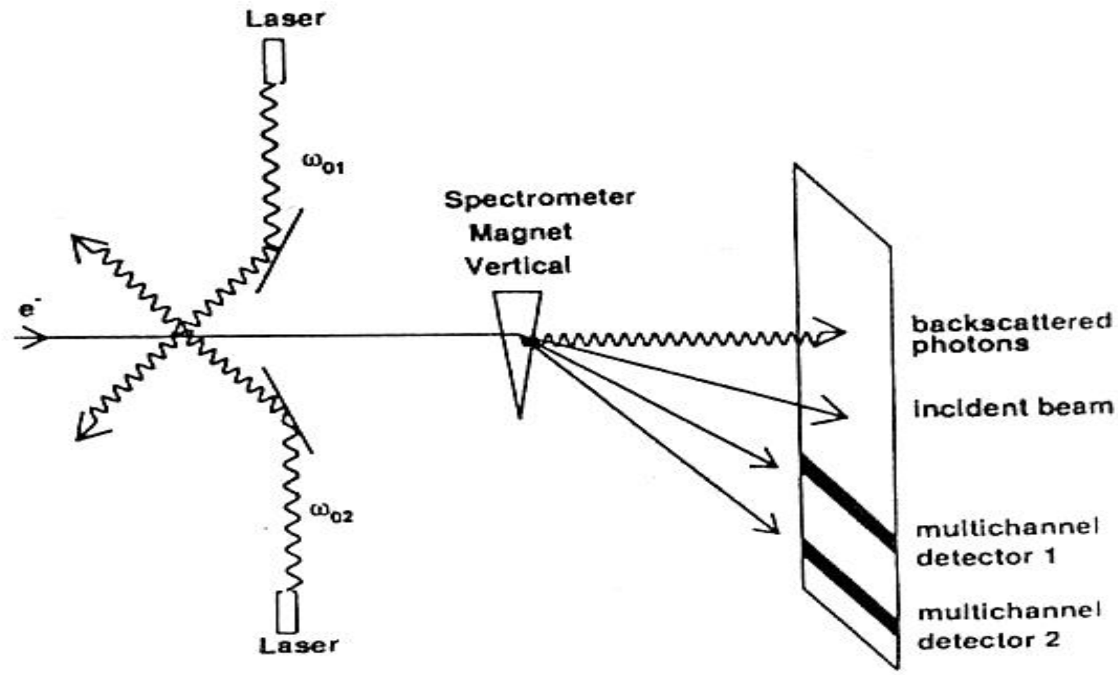

Fig. 17. The conceptual design of the experimental setup (depicted from [29]).

Let us consider in more details the case, when the coordinates of the center of magnetic field is not known. In this case to determine the bending angles of recoil electrons two rows of monitors, mounted on a precision optical table, would be used. If the distance between the front and rear monitors is $c_1$and distances between the centroids of the forward scattered photon beam and recoil electrons on the front and rear monitors a_1 and b_1 respectively, then the bend angle is $\vartheta = (a_1 - b_1)/c_1$, and

$$\frac{d\vartheta}{\vartheta} = \sqrt{\frac{(da_1)^2+(db_1)^2}{(a_1-b_1)^2} + \left(\frac{dc_1}{c_1}\right)^2} \tag{4.12}$$

For $a_1 = 0.8m$, $b_1 = 1.2m$, $c_1 = 2.0m(\vartheta = 8.6^o)$ and $da_1 = db_1 = dc_1 = 15\mu$ this gives

$$\frac{d\vartheta}{\vartheta} = 7.1 \times 10^{-5}$$

Therefore the centroid of the forward scattered photon beam and the positions of the recoil electrons on the two rows of monitors must be determined to the level of 15μ.

The above requirement implies high resolution position monitors for recoil electrons as well as accurate measurement of the relative position of each monitor on the optical table. Regarding the centroid measurement of the forward scattered photons, the required photon detector must have good position resolution but need not measure the photon energy. One may use a detector consisting of a series of tungsten converter foils each followed by a pair of $x - y$ silicon μ-strip. With such a detector a detection efficiency is about 50% and a position resolution is about 12μ is feasible [41].

For the recoil electron beam, the μ-strip silicon or gaseous detectors seems promising. The resolution quoted for these devices is about 10μ. One of the main problems is that the backscattered photons have a fairly large angular spread. One must determine the centroid width much greater accuracy than this width.

The width of the angular distribution of backscattered photons in radians, is about $1/\gamma$, when the energy of photons not determined. With a beam energy of 5.0 GeV the width is 100 μ rad. It is conceivable that the centroid angle can be measured to within roughly 1/10 of the width. Since our requirement is 7 microrad, this is not problematic if the transverse dimensions of the incident beam of the order or lesser than 100μ and 30μ in the case of first (when center of magnetic field is known) and second (when center of magnetic field is not known) cases, respectively.

The angular and energy divergence of the incident beam influence on the energy resolution of the each individual events. As follows from the Monte Carlo simulations, the absolute value of mean energy of the beam can be determined within and order of magnitude better than the energy spread of the recoil electrons. At the GRAAL the Compton Edge was determined with in error of about 3μ for a statistics of 10^6 counts. At JLAB such a resolution can be achieved with less statistics, becouse the energy resolution of the tagging systen at JLAB is expected to be much better.

References

1. A. Einstein, NeueExperimenteüber den Einfluβ der Erdbewegung and die LichtgeschwindigkeitrelativzurErde, Forsch. UndFortschritte, 3, 36, 1927.
2. R. F. C. Vessot, M. W. Levine, E. M. Mattison, E. L. Blomberg, T. E. Hoffman, G. U. Nystrom, B. F. Farrel, R. Decher, P. B. Eby, C. R. Baugher, J. W. Watts, D. L. Teuber, and F. D. Wills, Test of Relativistic Gravitation with a Space-Borne Hydrogen Maser, Phys.Rev.Lett. 45, 2081, 1980.
3. E. Riis, L-U. A. Andersen, N. Bjerre, O. Poulsen, S. A. Lee, and J. L. Hall, Test of the Isotropy of the Speed of Light Using Fast-Beam Laser Spectroscopy, Phys.Rev.Lett. 60, 81, 1988.
4. Z. Bay, J. White, Comment on Test of the Isotropy of the Speed of Light, Phys.Rev.Lett. 62, 841, 1989.
5. S. Herrmann , A. Senger, E. Kovalchuk, H. Müller, A.Petersetal, Test of the Isotropy of the Speed of Light Using a Continuously Rotating Optical Resonator, Phys. Rev. Lett. 95,150401, 2005.
6. P. Antonini, M. Okhapkin, E. Göklü, and S. Schiller, Test of constancy of speed of light with rotating cryogenic optical resonators, Physical ReviewA71, 050101, 2005.
7. M. A. Hohensee, P. L. Stanwix, M. E. Tobar, S. R. Parker, D. F. Phillips, R. L. Walsworth, Improved constraints on isotropic shift and anisotropies of the speed of light using rotating cryogenic sapphire oscillators", *Physical Review D***82**, 076001, 2010.
8. V.A. Kostelecky, Gravity, Lorentz violation, and the standard model, Phys. Rev. D. 2004. – 69, 105009, 2004.
9. D. Mattingly, Modern Tests of Lorentz Invariance, Living Rev. Relativity,8, 5, 2005.
10. V.A. Kostelecky, N. Russell, Data Tables for Lorentz and CPT Violation,Reviews of Modern Physics,83, 2011.
11. BICEP2 Collaboration:P.A.R. Ade, R. W. Aikin, D. Barkats, S. J. Benton, C. A. Bischoff, J. J. Bock, J. A. Brevik, I. Buder, E. Bullock, C. D. Dowell, L. Duband, J. P. Filippini, S. Fliescher, S. R. Golwala, M. Halpern, M. Hasselfield, S. R. Hildebrandt, G. C. Hilton, V. V. Hristov, K. D. Irwin, K. S. Karkare, J. P. Kaufman, B. G. Keating, S. A. Kernasovskiy, J. M. Kovac, C. L. Kuo, E. M. Leitch, M. Lueker, P. Mason, C. B. Netterfield, H. T. Nguyen, R. O'Brient, R. W. Ogburn IV, A. Orlando, C. Pryke, C. D. Reintsema, S. Richter, R. Schwarz,

C. D. Sheehy, Z. K. Staniszewski, R. V. Sudiwala, BICEP2 I: Detection Of B-mode Polarization at Degree Angular Scales, arXiv:1403.3985

12. C. R. Contaldi, M. Peloso, L. Sorbo, Suppressing the impact of a high tensor-to-scalar ratio on the temperature anisotropies, arXiv:1403.4596
13. V.G. Gurzadyan, A.T. Margarian, Inverse Compton testing of fundamental physics and the cosmic background radiation, Physica Scripta, 53, 513, 1996.
14. V.G. Gurzadyan, J.P. Bocquet, A.Kashin, A.Margarian, O.Bartalini, V.Bellini, M.Castoldi, A.D'Angelo, J.-P.Didelez, R.Di Salvo, A.Fantini, G.Gervino, F.Ghio, B.Girolami, A.Giusa, M.Guidal, E.Hourany, S.Knyazyan, V.Kouznetsov, R.Kunne, A.Lapik, P.LeviSandri, A.Lleres, S.Mehrabyan, D.Moricciani, V.Nedorezov, C.Perrin, D.Rebreyend, G.Russo, N.Rudnev, C.Schaerf, M.-L.Sperduto, M.-C.Sutera, A.Turinge, Probing the Light Speed Anisotropy with respect to the Cosmic Microwave Background Radiation Dipole, Mod. Phys. Lett. A, 20,1, 2005.
15. V.G. Gurzadyan, J.P.Bocquet, A.Kashin, A.Margarian, O.Bartalini, V.Bellini, M.Castoldi, A.D’Angelo, J.-P.Didelez, R.Di Salvo, A.Fantini, G.Gervino, F.Ghio, B.Girolami, A.Giusa, M.Guidal, E.Hourany, S.Knyazyan, V.Kouznetsov, R.Kunne, A.Lapik, P.LeviSandri, A.Lleres, S.Mehrabyan, D.Moricciani, V.Nedorezov, C.Perrin, D.Rebreyend, G.Russo, N.Rudnev, C.Schaerf, M.-L.Sperduto, M.-C.Sutera, A.Turinge, Lowering the Light Speed Isotropy Limit: European Synchrotron Radiation Facility Measurements, NuovoCimento, 122, 515, 2007.
16. J.-P. Bocquet, D. Moricciani, V. Bellini, M. Beretta, L. Casano, A. D'Angelo, R. Di Salvo, A. Fantini, D. Franco, G. Gervino, F. Ghio, G. Giardina, B. Girolami, A. Giusa, V.G. Gurzadyan, A. Kashin, S. Knyazyan, A. Lapik, R. Lehnert, P. Levi Sandri, A. Lleres, F. Mammoliti, G. Mandaglio, M. Manganaro, A. Margarian, S. Mehrabyan, R. Messi, V. Nedorezov, C. Perrin, C. Randieri, D. Rebreyend, N. Rudnev, G. Russo, C. Schaerf, M.L. Sperduto, M.C. Sutera, A. Turinge, V. Vegna, Limits on light-speed anisotropies from Compton scattering of high-energy electrons, Phys.Rev.Lett.104:241601, 2010.
17. V.G. Gurzadyan, V. Bellini, M. Beretta, J.-P. Bocquet, A. D'Angelo, R. Di Salvo, A. Fantini, D. Franco, G. Gervino, G. Giardina, F. Ghio, B. Girolami, A. Giusa, A. Kashin, H.G. Khachatryan, S. Knyazyan, A. Lapik, P. Levi Sandri, A. Lleres, F. Mammoliti, G. Mandaglio, M. Manganaro, A. Margarian, S. Mehrabyan, R. Messi, D. Moricciani, V. Nedorezov, D. Rebreyend, G. Russo, N. Rudnev, C. Schaerf, M.-L. Sperduto, M.-C. Sutera,

A. Turinge, V. Vegna, A new limit on the light speed isotropy from the GRAAL experiment at the ESRF, Proceed. XII M. Grossmann meeting on General Relativity, World. Sci., vol. B, p.1495, 2012.; arXiv:1004.2867

18. C.L. Bennett et al, Nine-Year Wilkinson Microwave Anisotropy Probe (WMAP) Observations: Final Maps and Results, ApJS, 208, 20, 2013
19. S. Rauzy, V.G. Gurzadyan, On the motion of the Local Group and its substructures, Mon. Not. Roy. Astr. Soc., 298, 114, 1998.
20. M.F. Ahmed, B.M. Quine, A. Sargoytchev, S.Stauffer, A. D.,A review of one-way and two-way experiments to test the isotropy of the speed of light, I. Journ. Phys., 86, 835, 2012.
21. L. Lingli, B. Ma, A theoretical diagnosis on light speed anisotropy from GRAAL experiment, Astroparticle Phys., 36, 37, 2012.
22. M. Cambiaso, Lehnert R., Potting R., Massive Photons and Lorentz Violation, Phys. Rev. D, 85, 085023, 2012.
23. V.A. Kostelecky, D. Mewes, Electrodynamics with Lorentz-violating operators of arbitrary dimension, Phys. Rev. D. 80, 015020, 2009.
24. B. Audren, D. Blas, J. Lesgourgues, S. Sibiryakov, Cosmological constraints on Lorentz violating dark energy, Journal of Cosmology and Astroparticle Physics, 08, id. 039, 2013.
25. B. Audren, D. Blas; M. M. Ivanov, J. Lesgourgues, S. Sibiryakov, Cosmological constraints on deviations from Lorentz invariance in gravity and dark matter, arXiv:1410.6514, 2014.
26. S. Ando, M. Kamionkowski, and I. Mocioiu, Neutrino Oscillations, Lorentz/CPT Violation, and Dark Energy, Phys.Rev. D80, 123522,2009
27. C. Zhe, S. Wang, Constraints on space time anisotropy and Lorentz violation from the GRAAL experiment, Eur. Phys. J. C, 73, 2337, 2013.
28. I. Ginzburg et al. Colliding gamma e and gamma gamma Beams Based on the Single Pass Accelerators (of Vlepp Type), Nucl. Instr. Meth. 205, 47, 1983.
29. S. Knyazian, A. Margarian, S. Mehrabyan. Compton Edge electron beam spectrometer, Preprint YerPhi 1486(3)-97, 1997.
30. P. Chvetsov, A. Day, J.-C. Denard,A. P. Freyberger, R. Hiks. Non-invasive energy spread monitoring for the JLAB experimental program via synchrotron light interferometers, Nucl. Instr. & Meth. A557, pp 324-327 (2006).

31. S. Watson et al., Precision measurements of the SLC reference magnets. SLAC-PUB-4908 (1989)
32. C. Schaerf, The GRAAL Project; a polarized and tagged gamma-ray beam, Nuclear Phys. News (Europe) V2, n1 (1992) 7
33. Conceptual Design Report, CEBAF Basic Experiment Equipment, April 13, 1990
34. T. P. Welch and R. Ent, Energy measurement of electron beams by Compton scattering, CEBAF, unpublished (1994)
35. Michael J. Fero, The Compton Polarimeter for SLC, SLAC-PUB-6026 (1992)
36. F. R. Bouchet, The Planck mission, arXiv:1405.0439
37. Planck Collaboration: P. A. R. Ade, N. Aghanim, M. Arnaud, M. Ashdown, J. Aumont, C. Baccigalupi, et al, Planck intermediate results. XVI. Profile likelihoods for cosmological parameters, arXiv:1311.1657
38. V.G. Gurzadyan, P.A.R. Ade, P. de Bernardis, C.L. Bianco, J.J. Bock, A. Boscaleri, B.P. Crill, G. De Troia, K. Ganga, M. Giacometti, E. Hivon, V.V. Hristov, A.L. Kashin, A.E. Lange, S. Masi, P.D. Mauskopf, T. Montroy, P. Natoli, C.B. Netterfield, E. Pascale, F. Piacentini, G. Polenta, J. Ruhl, Ellipticity analysis of the BOOMERanG CMB maps, Int.J.Mod.Phys.D12, 1859, 2003.
39. V.G. Gurzadyan, A.L. Kashin, H. Khachatryan, E. Poghosian, S. Sargsyan, G. Yegorian , To the center of cold spot with Planck, Astron. &Astrophys.566, id.A135, 2014.
40. S.G. Djorgovski, V.G. Gurzadyan, Dark Energy From Vacuum Fluctuations, Nucl. Phys.B PS173, 6, 2007.
41. B. E. Norum, T. P. Welch, An Intense Polarized Source at CEBAF Hall B, CEBAF LOI 93-012, 1993.
42. D. Gaskell, High Precision Compton and Møller Polarimetry at Jefferson Lab, talk at PAVI14, July, 2014.